Proceedings of the 7th International Symposium on Cavitation
CAV2009
August 17-22, 2009, Ann Arbor, Michigan, USA

CAV2009 – Paper No. 66

Pressure-Wave Formation and Collapses of Cavitation Clouds Impinging on Solid Wall in a Submerged Water Jet

Keiichi SATO
Kanazawa Institute of Technology
Nonoichi-Machi, Ishikawa, Japan

Yasuhiro SUGIMOTO
Kanazawa Institute of Technology
Nonoichi-Machi, Ishikawa, Japan

Saburo OHJIMI
Shibuya Kogyo Co. Ltd.
Kanazawa, Ishikawa, Japan

ABSTRACT

A high-speed water jet ejected into water forms a cavitating water jet accompanied with cavitation clouds in a periodic manner. A powerful impulsive force can be caused at the collapse of unsteady cavitation clouds at the same time when the cavitating water jet impinges against a solid wall. It is known that this force can be widely used in an industrial field such as cleaning, cutting, and peening.

In the present experiment, cavitation clouds are observed to investigate the details such as impinging, dividing and collapsing behaviors using a constrained-type test section as well as an open-type test section. The constrained-type test section is used to quasi-two dimensionally observe the behavior of cavitation clouds in the near impinging wall region. The present purpose is to investigate about the behavior of cavitating water jet in the near impinging wall region as well as the relation of cavitation cloud collapse with the formation of pressure wave, the propagation of pressure wave and the cavitation impact.

In order to estimate the high speed phenomena such as rapid and consecutive collapses of cavitation clouds and pressure wave formation, the frame difference method for cavitating flow is used in the present image analysis for cavitation cloud. The usefulness of the method is experimentally verified for the behavior analysis of high speed liquid flow accompanied with growth and collapse of bubbly cloud.

As a result it is experimentally found that 1) the present image analysis method based on the frame difference method makes possible to grasp the motion of pressure wave propagation in cavitation cloud, 2) local cloud collapse causes a pressure wave which propagates toward the surrounding area and as a result causes secondary collapses in a chain-reaction manner, and 3) cavitation clouds on the impinging wall tend to be peripherally located in an annular zone at the final collapsing stage. The existence of the annular cloudy zone can be related to the ring-like cavitation erosion distribution and the chain-reaction-type propagation of cavitation clouds.

INTRODUCTION

In characteristics of cavitation phenomena the behavior of cavitation clouds plays an important role as well as the dynamics of individual bubbles. A typical example of strong impulsive cavitation cloud is caused by vortex cavitation in the shear layer of high speed submerged jet in water. According to many previous investigations [e.g. 1-4], the cavitating water jet forms periodically discontinuous cavitation clouds and produces strong impacts at the jet impingement or the cloud collapses. This impulsive force attracts an industrial attention from viewpoints such as cutting, peening and cleaning [5, 6].

It can be pointed out that cavitation clouds can form a strong pressure wave or shock wave depending on the internal condition of the cloud when the rapid collapse occurs as an inside contraction type [7]. According to the previous studies of the authors [8, 9], cavitation cloud shows rapid deformation and causes strong impacts at the collapse when a cavitating water jet impinges on the solid wall. It is predicted that a collapse of cavitation cloud produces consecutive collapses of clouds or bubbles [10] and forms a complex field of impulsive pressure pulses which can be related to impulsive, cutting and cleaning effects.

The purpose of the present study is to experimentally investigate the fundamental mechanism to produce such important effects from an industrial and academic viewpoint. A periodic unsteady water jet with cavitation clouds is examined by the observation experiments using a ultra-speed video camera and an image analysis based on the frame difference method for cavitating flow [11] to make clear the process of pressure wave formation due to discontinuous cavitation clouds in the near impinging wall region as well as the process of pressure wave propagation. In the present study it is found that the frame difference method based on the occurrence and disappearance of minute bubbles is very useful to visually analyze the phenomena accompanied with collapses of cavitation clouds such as a cavitating flow. In addition, in the case of cavitating water, a jet impinging on solid wall produces pressure waves in a consecutive manner and propagates to a surrounding direction to cause strong impact on the wall.

EXPERIMENTAL SET UP AND METHOD

Experiments

In the present study, experiments were conducted using two types of horn-type nozzles such as nozzle A and nozzle B as shown in Fig. 1. Both the nozzles had a similar structure with throat diameter of d=1mm and aperture angle of θ=60deg except for the length of horn part and the conduit diameter upstream of the nozzle throat. Tap water was used and issued into a downstream test section at atmospheric pressure P_2 under upstream pressure P_1=6MPa through a high pressure pump. Air content in test water was estimated as dissolved gas content β.

Two kinds of test sections were used where test section A was a normal open-type and test section B was a constrained type with the flow passage width of 5mm to quasi-two-dimensionally observe a bubble collapsing behavior in the near jet impinging wall region as shown in Fig. 2. Both the test sections had an impinging wall made of a transparent acrylic resin plate installed in the position of stand-off x/d=30 and

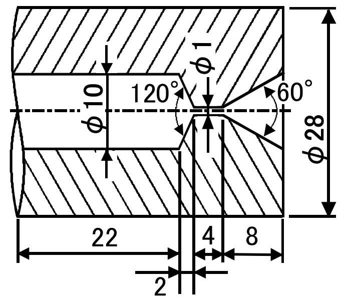

(a) Nozzle A

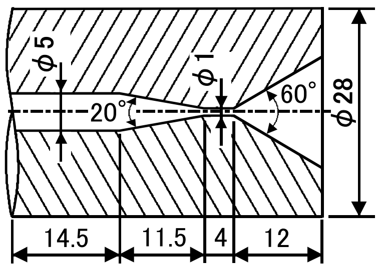

(b) Nozzle B

Figure 1: Two kinds of horn nozzles

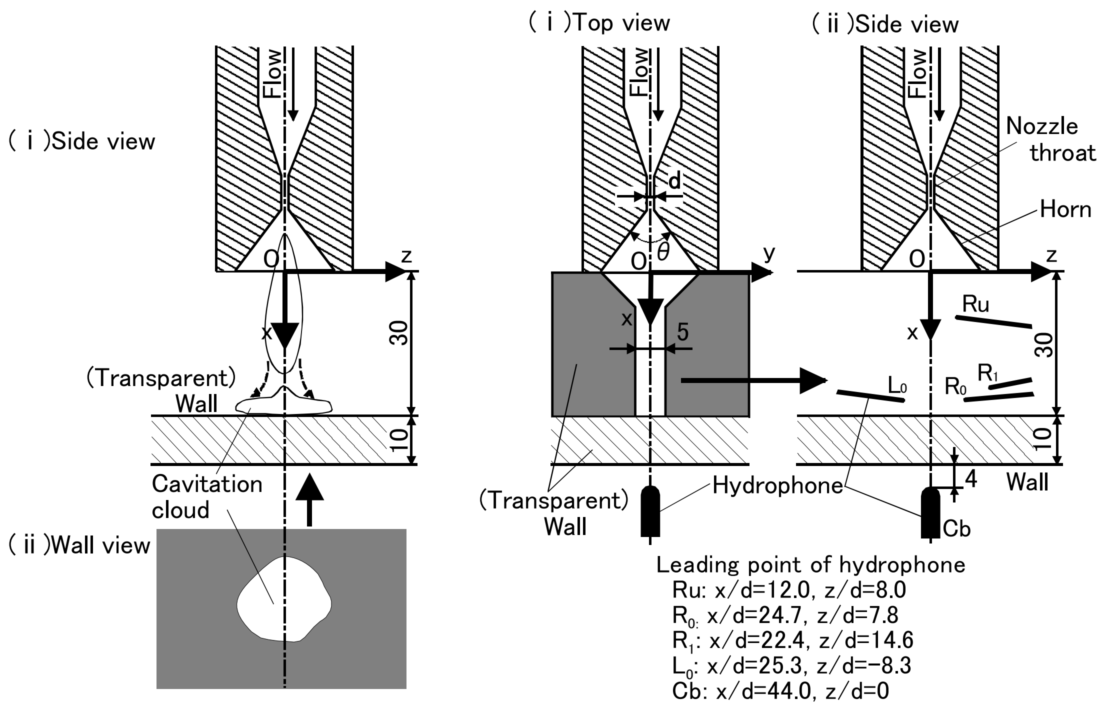

(a) Test section A (b) Test section B

Figure 2: Two types of test sections downstream of nozzle

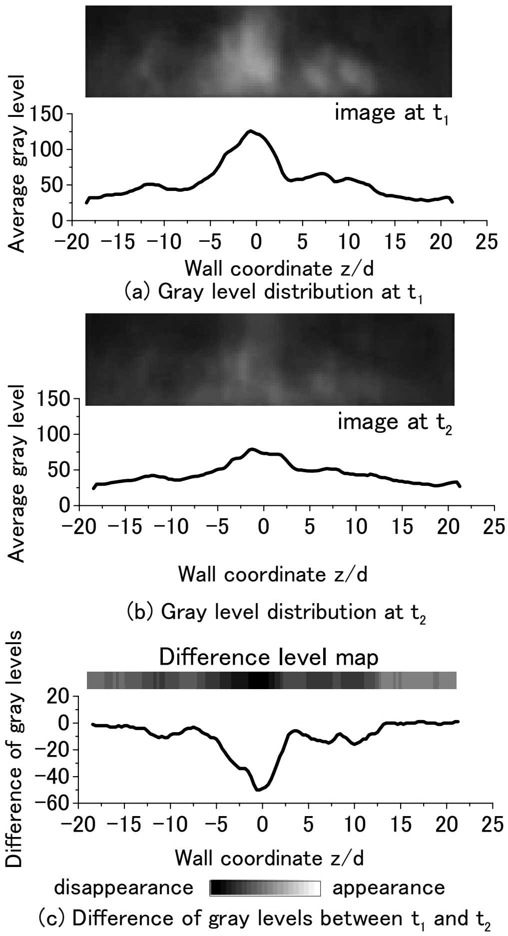

Figure 3: Image analysis using frame difference method for cavitating flow

normal to a center axis of the nozzle. The exit of horn part in the nozzle was chosen as the original point, the direction of nozzle center axis as x-axis, and the directions normal to it as y or z-axis along the impinging wall surface.

In order to examine the impulsive characteristics, some hydrophones (B&K; 8103 and Muller; Platte Needleprobe) were installed inside the test section and in the backside of the impinging wall depending on the experimental conditions. The hydrophones were named as Ru, R_0, R_1, L_0 and Cb depending on the installation position as shown in Fig. 2(b), respectively.

Video observation and image analysis for cavitating flow

The behavior of cavitation clouds was observed using two kinds of high speed video cameras (Kodak; Model HS4540 and Photron; FASTCAM SA1) with three kinds of frame speeds Fs=27000, 54000 and 100000fps. Air content in test water was measured in the term of dissolved oxygen content.

The frame difference method for cavitating flow [11] is used in the present image analysis for cavitation cloud. The usefulness of the method is experimentally verified for the behavior analysis of high speed liquid flow accompanied with growth and collapse of bubbly cloud as shown in the present study. The outline of the method is shown in Fig. 3. Figure 3(a) shows a gray level averaged in the vertical direction of the image at time t_1 and also Fig. 3(b) at time t_2. In the image the white colored portion corresponds to a cluster of minute bubbles, namely cavitation cloud. Thus Fig. 3(c) shows the difference between the former image of Fig. 3(a) and the latter image of Fig. 3(b) at the time interval $\Delta t=t_2-t_1$. From the result of Fig. 3(c) we can find the line or zone where the gray level changes rapidly which means cavitation cloud rapidly disappears or appears. Through the frame difference analysis in the range of observation, we can obtain the final image analysis for cavitating flow field.

In the present analysis, the appearance region of cloud is colored as a white and the disappearance region as a black. It, in general, should be noted that high-speed phenomena are relatively clear in the view of high speed movie (namely, motion pictures) but becomes little clear in the view of still pictures because of the information shortage on the change rate of images. Through the process of the present image analysis we can quantitatively estimate the high speed phenomena such as rapid and consecutive collapses of cavitation clouds and pressure wave formation.

EXPERIMENTAL RESULTS

Measurement of pressure wave propagation in cavitation cloud

Figure 4(a) shows an observation result using a high speed video camera for collapsing behavior of cavitation clouds of the near impinging wall region in the test section B. In this section, as the first step, the effectiveness of the analysis is presented about the image analysis based on the frame difference method which is used for the high speed video observation in this study. The details of the formation of pressure wave and the propagation process will be discussed in the next section.

In Fig. 4(a) the appearance of cavitation cloud in the near impinging wall region is shown using back lighting at a frame speed of 100000fps. The area of observation is a rectangular zone of 47 x 15mm. The lapsed time tp for observation is depicted in the right side of each picture. In the pictures there are some black shadows of cavitation clouds as well as three hydrophones to measure sound pressure in water. The gray level in the picture changes, when minute bubbles in water appear and disappear due to the influence of the pressure field and also move due to the velocity field. Therefore through the variation of the gray level in the picture it is possible to analyze the pressure and velocity field. The point is to grasp the change rate of the gray level.

In the present study, the analysis for the pressure and/or velocity field with a time-dependent and locally fluctuating state was quantitatively made by the frame difference method using a temporal gradient of gray level in the images taken with a high speed video camera. From the results in Fig. 4(c), it is found that a black colored band extends to an oblique downward direction from point-A. This means that the pressure wave occurring in region-A propagates to the surrounding area. The propagation speed to the right direction can be estimated to be about 170m/s since the gradient of the band means the translational speed as shown by the dotted line in Fig. 4(c). The value is valid as the pressure propagation because of the existence of void in water. On the other hand the points of R_0

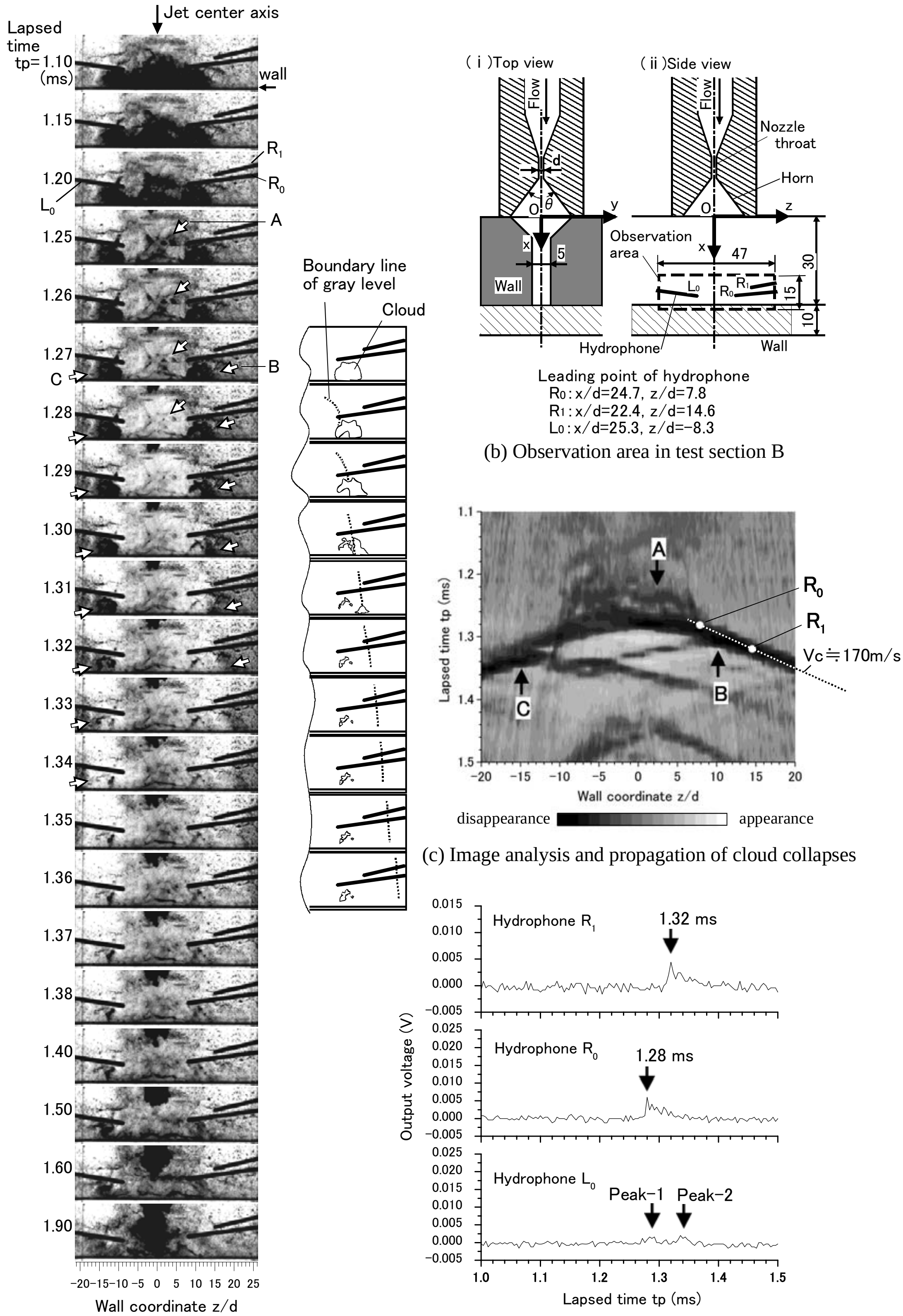

(a) Collapsing behavior of cavitation cloud in jet peripheral zone

(b) Observation area in test section B

(c) Image analysis and propagation of cloud collapses

(d) Sound pressure measured with hydrophones R_0, R_1 and L_0

P_1=6MPa, P_2=0.1MPa, Tw=292K, β=5.3mg/ℓ, d=1mm, x/d=30, Fs=100000fps

Figure 4: Jet peripheral type of collapsing behavior of cavitation cloud in near impinging wall region (horn nozzle B, test section B, tp=lapsed time[ms], Tw=water temperature)

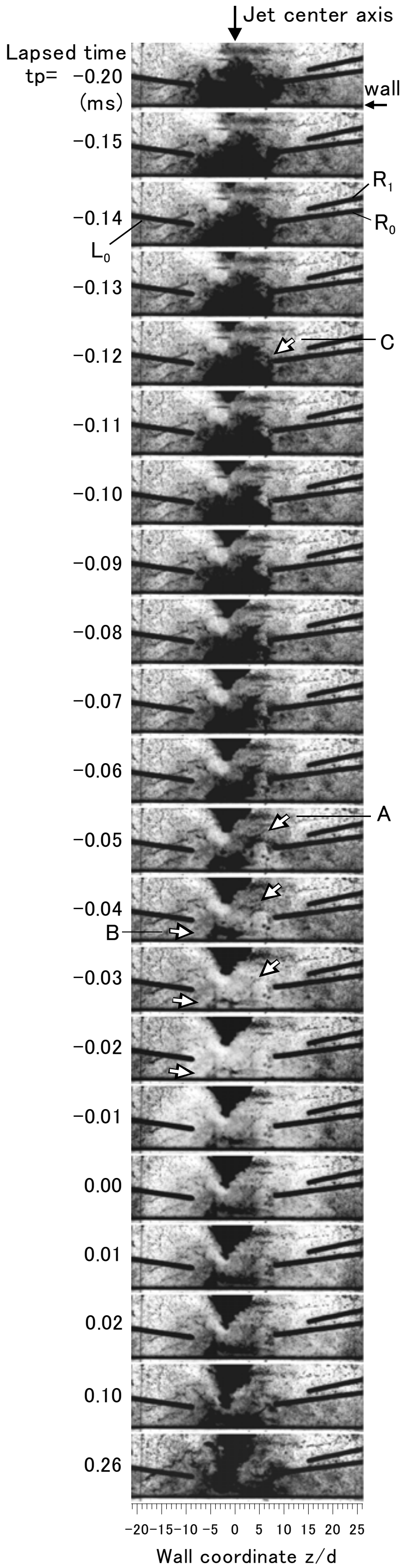

(a) Collapsing behavior of cavitation cloud in jet center-axis zone

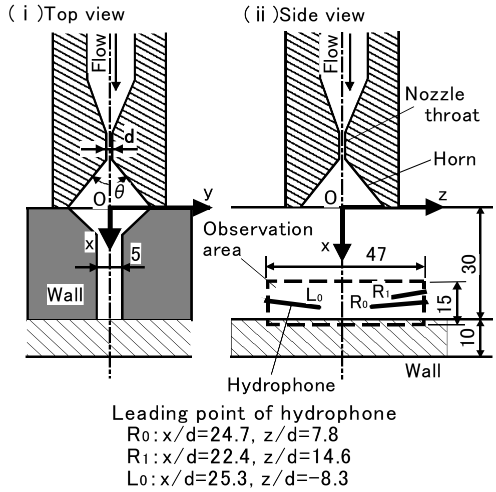

(b) Observation area in test section B

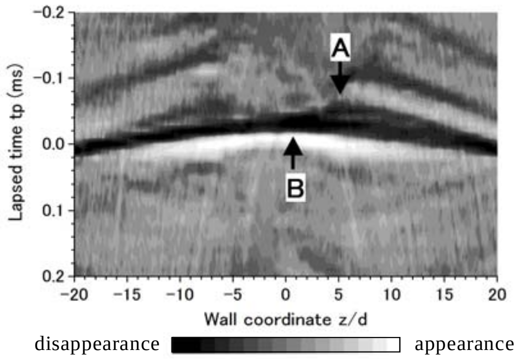

(c) Image analysis and propagation of cloud collapses

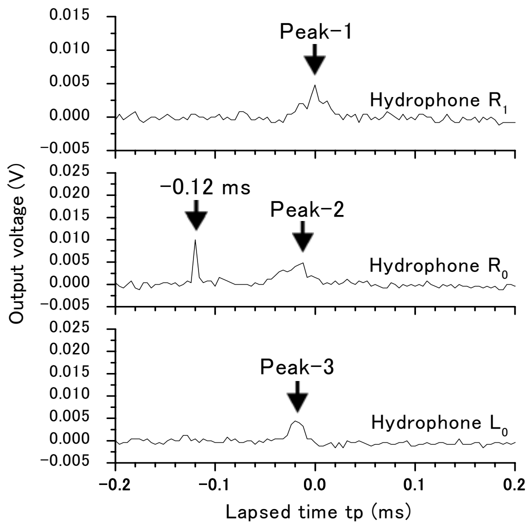

(d) Sound pressure measured with hydrophones R_0, R_1 and L_0

P_1=6MPa, P_2=0.1MPa, Tw=292K, β =5.3mg/ℓ, d=1mm, x/d=30, Fs=100000fps

Figure 5: Jet center-axis type of collapsing behavior of cavitation cloud in near impinging wall region (horn nozzle B, test section B)

and R_1 in Fig. 4(c) correspond to the leading positions of microphones R_0 and R_1 as shown in Fig. 4(b), respectively. The results due to the measurement of sound pressure shown in Fig. 4(d) depict the arrival time of sound pressure around t_0=1.28ms in R_0 and t_1=1.32ms in R_1, where these times are in good agreement with the lapsed times on the vertical axis in Fig. 4(c). The propagation speed can be also estimated to be 170m/s because the time interval Δt=0.04ms and the space interval between the hydrophones is Δs=6.8mm so that the value exactly agrees with that of the gradient in Fig. 4(c). The propagation of pressure is also optically confirmed on the images because it can be observed from Fig. 4(a) that the boundary line in which the gray level rapidly changes passes the microphone R_0 around the lapsed time of tp=1.28ms and the microphone R_1 around the lapsed time of tp=1.32ms. In addition there are two peaks by the hydrophone L_0 in Fig. 4(d) where it can be pointed out that the peak-1 around tp=1.29ms corresponds to the pressure wave due to the collapse-A and the peak-2 around tp=1.34ms corresponds to that due to the collapse-C.

From the results mentioned above it is found that the frame difference method using the time rate of gray level in the images taken in bubbly flow region is very effective on the quantitative analysis of propagation behavior of pressure wave. In Fig. 4(c) presenting the analysis result, by the way, it should be noted that the many vertical and thin streaks in the whole image mean the translational motion of minute bubbles or clouds in the velocity field.

Collapsing behavior of cavitation clouds and pressure wave formation in near impinging wall region

In the preceding section the effectiveness of the frame difference method is shown on a cavitating and bubbly flow using the results in Fig. 4. Based on the same results, here, the collapsing behavior of cavitation clouds is discussed in the near impinging wall region. First, in the case of an example shown in Fig. 4(a), cavitation clouds on the impinging wall around tp=1.10ms disappear step by step with a lapse of time under the influence of pressure field and then around the lapsed time of tp=1.25 to 1.28ms the primary collapse occurs in the region centered by the jet center axis and at a distance from the wall surface as shown by the arrow-A in Fig. 4(a). At this time it is found that there are a pair of wall-attached type clouds shown by the arrows-B and C in the peripheral zone of cavitating jet which are located around z/d=±5 to ±15, in addition to a leading part of new cavitating jet around the jet center axis in the upper edge of the picture. These two attached-type clouds collapse in a chain-reaction manner [10] due to the influence of the pressure propagation caused by the primary collapse of cloud-A around tp=1.31ms and 1.34ms respectively so that the two cloud collapses also cause two new pressure propagations as shown in Fig. 4(c).

The collapses of wall attached-type clouds caused by the pressure propagation in the near impinging wall region should be noticed from the standpoint of cavitation impact and erosion. The collapses occur in the peripheral zone of cavitating jet and can be related to the ring-like erosion pits distribution which is well known as a typical erosion distribution of cavitating water jet. A typical erosion distribution in the experimental set-up (test section B) will be shown in the appendix-B.

Figure 5(a) shows another typical example of collapsing behavior of cavitation cloud in the near impinging wall region. Figures 5(c) and 5(d) also show the result of image analysis based on the frame difference method for the images in Fig. 5(a) and the result of measurement of sound pressure, respectively.

First of all, around an arbitrary lapsed time of t=-0.20ms there is also a relatively large cavitation cloud. In a similar manner with the result of Fig. 4 mentioned before, the cavitation cloud disappears step by step due to the surrounding pressure with a lapse of time. Though in Fig. 5(d) there is a sharp peak of sound pressure around tp=-0.12ms measured with the microphone R_0, this peak is caused by a local cavity collapse near the microphone R_0 as shown by the arrow-C. In this example the primary collapse-A is caused around the time of tp=-0.05 to -0.03ms in a distance from the wall surface near the jet center axis. And the following position of cloud collapse is at the location-B of the jet center axis near the primary collapse. The relation of the primary collapse-A with the next collapse-B is not clear in this case. The peaks-1, 2 and 3 as shown in Fig. 5(d) are caused by the arrivals of the pressure waves at the positions of hydrophones R_1, R_0 and L_0, where the peak-2 is around the peak range of tp=-0.04 to 0ms.

Therefore the location of cloud collapse in the near impinging wall region appears to be divided into two parts such as the jet peripheral zone and the jet center-axis zone.

Shedding and impinging process of periodic cavitating water jet, including near impinging wall region

In the constrained test section B a typical example of the result is shown in Fig. 6 where the whole appearance of cavitation cloud impinging on the wall is observed from the instant of jet issue with a frame speed of Fs=54000fps. Two kinds of hydrophones are installed inside of the test section (hydrophone-Ru; measurement location x/d=12, y/d=0, z/d=8) and behind the impinging wall (hydrophone-Cb; measurement location x/d=44, y/d=0, z/d=0) to measure the sound pressure together with the appearance observation of cavitation clouds. From the observation result of Fig. 6 it is confirmed that the cavitating water jet in the constrained test section B used in the present experiment has also a periodic unsteady shedding motion, though it is widely known that a cavitating water jet in general has a periodic behavior. In addition the comparison of the appearance will be made later between the open-type test section A and the constrained-type test section B (see, appendix-A) and the mechanism of periodicity will be explained in the next paper [12].

The main point is the behavior of cavitation cloud in the near impinging wall region. First, as shown at tp=-1.926ms in Fig. 6 it is found that there is a discontinuous portion of shedding cavitation cloud downstream of the nozzle horn exit (see, white arrow in the picture). The shedding appears to be periodic because the cloud discontinuous region periodically appears such as around tp=-1.926, -1.037 and -0.296ms. The image analysis for these images is shown in Fig. 7(a) using the frame difference method where the difference interval is one frame. The result in Fig. 7(a) depicts the change rate of

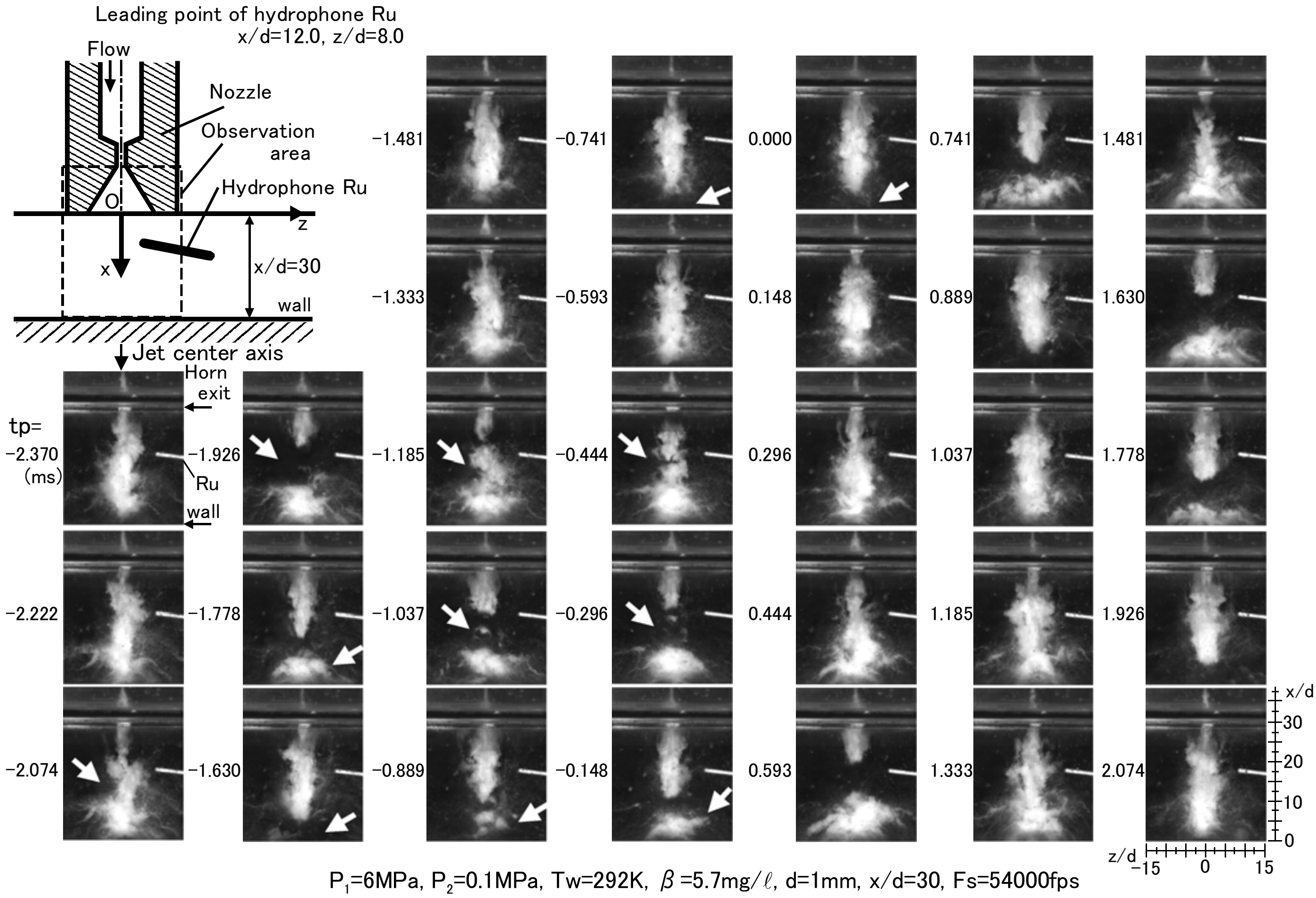

Figure 6: Observation of cavitating water jet in test section B (test section B, horn nozzle A)

cavitation cloud motion along the direction of jet axis (x-axis). Figure 7(b) shows the result of sound pressure measured at the same time with the high speed video observation. The scales in the horizontal axes are coincident with each other between Fig. 7(a) and Fig. 7(b).

In Fig. 7(a) the black part represents the region of cloud disappearance and the white part represents the region of cloud appearance. It is found that a white band extends from the nozzle to the near impinging wall region. The band corresponds to the translational motion of cavitating water jet which is issued from the nozzle and flows at a high speed toward the wall. It keeps almost straight though it curves gently near the wall since the speed of the leading part of cavitating jet decreases near the wall. The speed is about Vp=60 to 65 m/s in the straight part from the nozzle. On the other hand it is found that there is a clear black area in the downstream region. This black band extending to the downstream from the location approximately x/d=10 depicts the movement or enlargement of the discontinuous zone in cavitation clouds. The high gradient means the rapid movement toward the wall. This translational movement shown by the black band is considered to be a vanishing motion of cavitation cloud caused by the propagation of high pressure because the propagation speed of the cloud discontinuous region is estimated to be a higher value of 2 or 3 times compared with the translational speed Vp of cavitating jet though the estimated value has some scatters. The starting area of the black colored band is located near the sound pressure peak measured by hydrophone-Ru as shown in Fig. 7(b).

The black colored band changes in the near impinging wall region of x/d=20 to 30 and then moves toward the wall together with some vertical black lines which mean the occurrence of high pressure waves. The behavior in the near impinging wall region is considered to be a propagation of small-scale collapses toward the wall in a chain-reaction manner. The collapse in the final stage generates the rapid line in an upstream direction, namely a clear upstream propagation of pressure wave as shown in Fig. 7(a). The period almost corresponds to that of pressure pulse measured by hydrophone-Cb.

In the near impinging wall region, it is found from these results that a series of cavitation clouds collapses and pressure wave occurrences are caused in a consecutive manner or a chain-reaction manner through a shrinking and collapsing

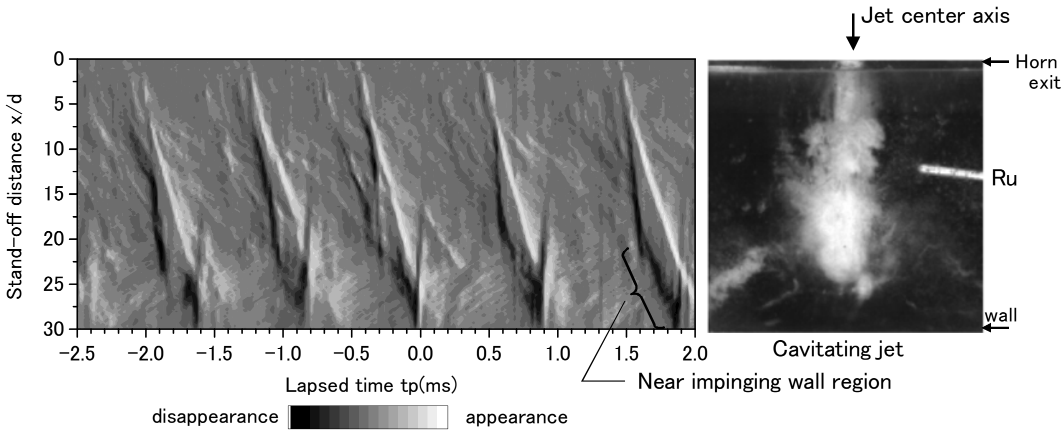

(a) Image analysis of cavitation cloud behavior in cavitating water jet

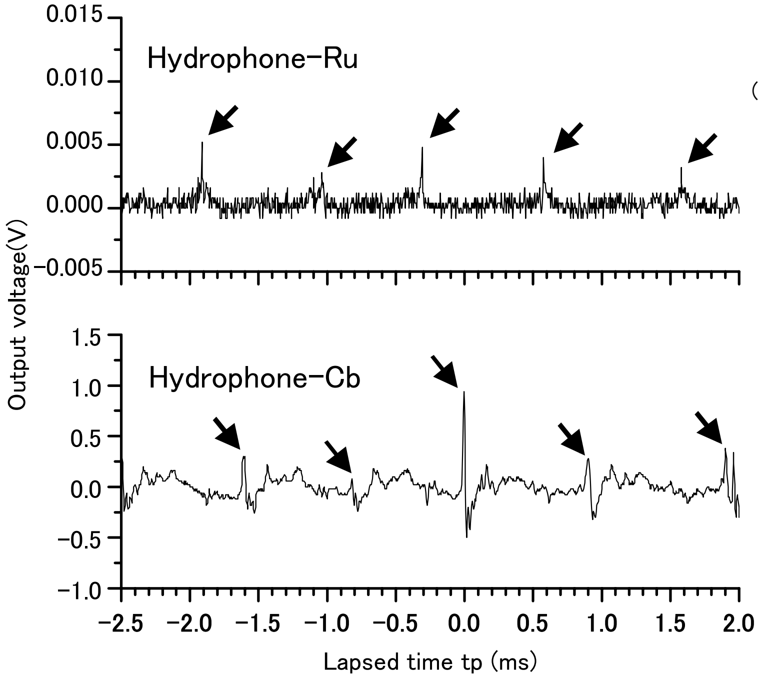

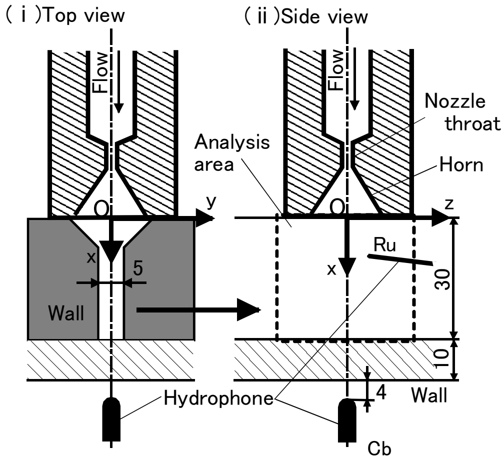

(c) Analysis area in test section B

(b) Sound pressure pulses

P_1=6MPa, P_2=0.1MPa, Tw=297K, β=5.7mg/ℓ, d=1mm, x/d=30, Fs=54000fps

Figure 7: Image analysis and output of hydrophones in test section B (horn nozzle A)

motion of cavitation cloud accompanied by the impinging motion of cavitating water jet toward the wall.

Collapsing behavior of cavitation clouds on impinging wall

Figure 8 shows the behavior of cavitation clouds on the impinging wall observed from the backside of transparent wall at a frame speed of 100000fps where the pictures are presented every 0.05ms. By the comparison with the nozzle configuration shown in Fig. 1 it is clear that a larger circle in the picture corresponds to the outer nozzle contour of 28mm in diameter and a smaller circle to the inside contour of 14mm in diameter. The lapsed time of observation is described at the left side where the original in time is arbitrary.

First of all, it is found from the picture at tp=0.10ms that there are a small white area-A in the center near the nozzle throat and a remaining cloud-B of the preceding cavitation cloud. The small area-A corresponds to the cavitation cloud just impinging on the wall since around this stage the leading part of cavitation cloud in cavitating water jet begins to appear as a clear white portion on the wall. Next with a lapse of observation time the white area of the impinging cavitation cloud-A centered in the picture enlarges step by step on the impinging wall. Around tp=0.25ms the peripheral clouds including the remaining cloud-B move outward with a shrinking motion and appear to be a string-like vortex cavity

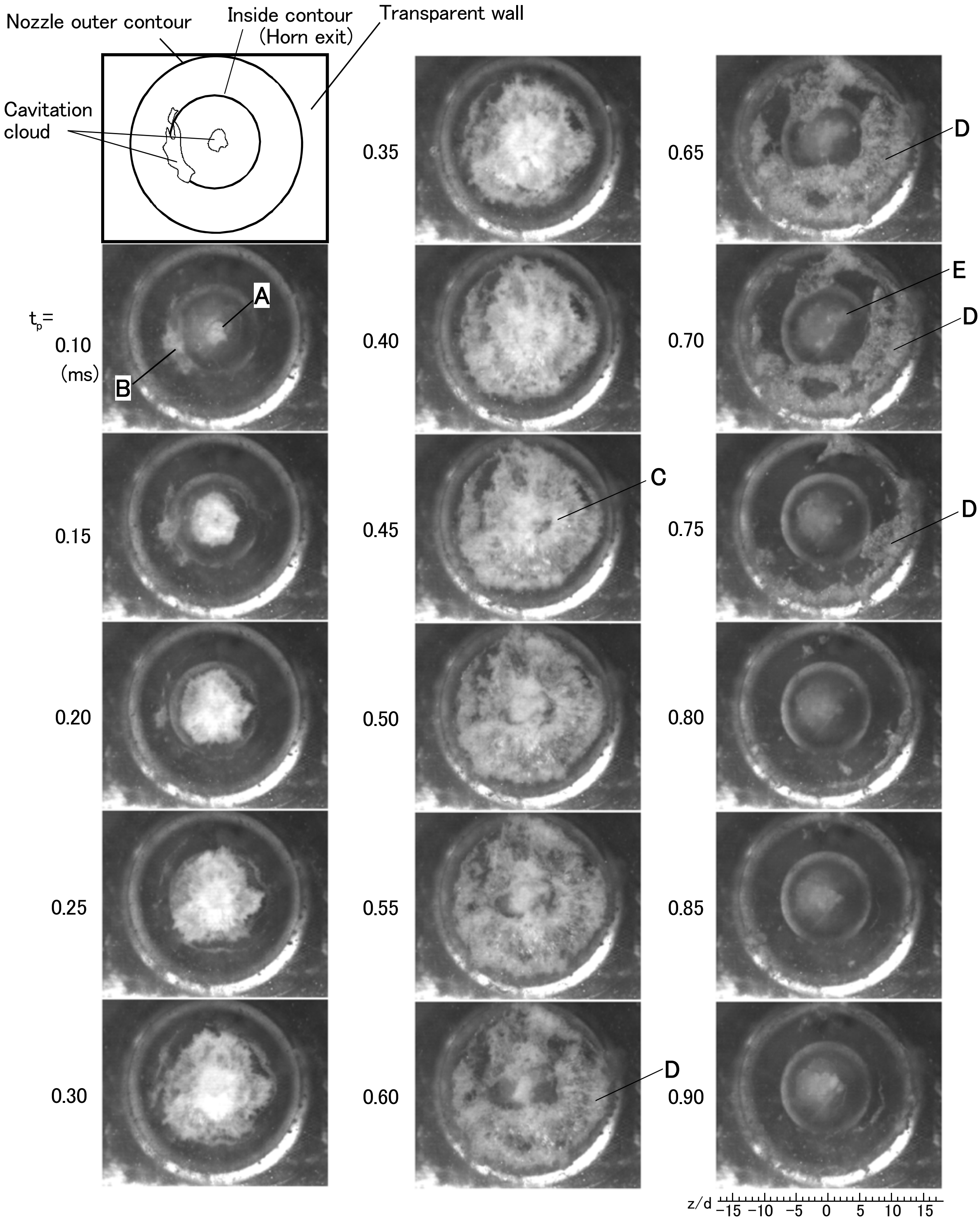

P_1=6MPa, P_2=0.1MPa, Tw=291K, β=5.1mg/ℓ, d=1mm, x/d=30, Fs=100000fps

Figure 8: Behavior of cavitation clouds on impinging wall (test section A, horn nozzle B)

with an axis parallel to the wall surface where it may be necessary to discuss the relation between this type of ring-like vortex bubble and the erosion mechanism [3, 13]. Though the impinging cavitation cloud-A further develops to a radial direction, around tp=0.45ms the cloud vanishing area-C begins to appear near the center of the large cloud region on the wall and rapidly expands to the whole direction to form an annular cloudy zone-D around tp=0.60 to 0.70ms. The formation of the annular area is considered to be in agreement with the cloud collapses in the near impinging wall region as mentioned in the preceding sections. Around these lapsed times a little obscure white portion-E in the center location indicates that of new cavitating jet approaching to the wall.

In the time range of tp=0.70 to 0.80ms it should be noticed that the annular cloud zone-D rapidly shrinks and collapses. The relation with the strong impact and erosion due to cavitation is pointed out about the behavior because the location of collapsing and vanishing clouds in the annular zone is in good agreement with a ring-like erosion distribution located around $z/d=\pm5$ to ±15 as shown in appendix-B. Though in the near impinging wall region there are two patterns of collapsing locations such as a jet center axis region and a jet peripheral region, the rate and the strength of cloud collapses on the impinging wall at the collapsing stage appears to be higher in the case of the jet peripheral region as shown in Fig. 8.

CONCLUSION

Cavitating water jet has a periodic unsteady behavior of cavitation clouds and causes a strong impact and erosion on the impinging wall surface. In the present study the cavitating water jet issued from a horn-type nozzle is observed with a high speed video camera and analyzed with the frame difference method for a cavitating flow. The main results are summarized as follows.

1) The present image analysis method based on the frame difference method makes possible to grasp the occurrence and disappearance of minute bubbles in cavitation cloud and is more effective on the motion analysis of pressure wave propagation in cavitation cloud.

2) Inside of large cavitation cloud in the near impinging wall region the local cloud collapses cause pressure wave which propagates toward the surrounding area and as a result causes successive collapses in a chain-reaction manner.

3) Cavitation clouds on the impinging wall caused by cavitating water jet tend to be peripherally located in the annular zone at the final collapsing stage. This annular location can be related to a ring-like erosion distribution on the impinging wall.

In this experiment, the stand-off is chosen to be 30d where it is measured from the exit of nozzle horn to the impinging wall and d depicts the throat diameter of nozzle. In addition the stand-off of 30d means a typical ring-like erosion distribution as shown in appendix-B.

REFERENCES

[1] Yamaguchi, A. and Shimizu, S. 1987, "Erosion due to impingement of cavitating jet," *Trans. ASME, J. of Fluids Engineering*, 109, 442-447.

[2] Vijay, M. M., Zou, C., and Tavoularis, S. 1990, "A study of the characteristics of cavitating water jets by photography and erosion," *Proc. of Tenth International Conference*, *Jet Cutting Technology*, 37-67.

[3] Soyama, H., Yamauchi, Y., Adachi, Y., Shindo, T., Oba, R. and Sato, K. 1994, "High-speed cavitation-cloud observations around high-speed submerged water jets," *Proc. 2nd International Symposium on Cavitation*, 225-230.

[4] Hulti, E. A. F. and Nedeljkovic, M. S. 2008, "Frequency in shedding/discharging cavitation clouds determined by visualization of a submerged cavitating jet," *Trans. ASME, J. of Fluids Engineering*, 130, 021304, 1-8.

[5] Kalumuck, K. M. and Chahine, G. L. 2000, "The use of cavitating jets to oxidize organic compounds in water," *Trans. ASME, J. of Fluids Engineering*, 122, 465-470.

[6] Soyama, H., Park, J. D. and Saka, M. 2000, "Use of cavitating jet for introducing compressive residual stress," *Trans. ASME, J. of Manufacturing Science and Engineering*, 122, No. 2, 83-89.

[7] Reisman, G. E., Wang, Y.-C. and Brennen, C. E. 1998, "Observations of shock waves in cloud cavitation," *J. of Fluid Mechanics*, 355, 255-283.

[8] Saito, Y. and Sato, K. 2006, "Instantaneous behavior of cavitation clouds at impingement of cavitating water-jet," *Proc. of Sixth International Symposium on Cavitation, CAV2006*, on CD-ROM.

[9] Sato, K., Ohjimi, S. and Sugimoto, Y. 2009, "Collapsing and impulsive behavior of cavitation clouds on cavitating water-jet impinging on solid wall," *Trans. JSME*, 75, Ser. B, No.750, 47-56.

[10] Sato, K., Shimojo, S. and Watanabe, J. 2003, "Observations of chain-reaction behavior at bubble collapse using ultra high speed video camera," *Proc. of ASME Cavitation and Multiphase Flow Forum*, FEDSM2003-45002, 1-6, on CD-ROM.

[11] Saito, Y. and Sato, K. 2007, "Bubble collapse propagation and pressure wave at periodic cloud cavitation," *Proc. of 6th International Conference on Multiphase Flow*, ICMF 2007, No.S7_Tue_C_25, on CD-ROM.

[12] Sato, K. Sugimoto, Y. and Ohjimi, S., 2009, "Structure of periodic cavitation clouds in submerged impinging water-jet issued from horn-type nozzle," *Proc. of 9th Pacific Rim International Conference on Water Jetting Technology*, to be published.

[13] Sato, K. and Kondo, S. 1996, "Collapsing behavior of a vortex cavitation bubble near solid wall: spanwise-view study," *Proc. of ASME Cavitation and Multiphase Flow Forum*, FED-236, 485-490.

Appendix-A: Appearance of periodic cavitating water jet in constrained-type test section B in comparison with open-type test section A

In a part of the experiment a constrained-type test section B shown in Fig. 2(b) was used to clearly observe the

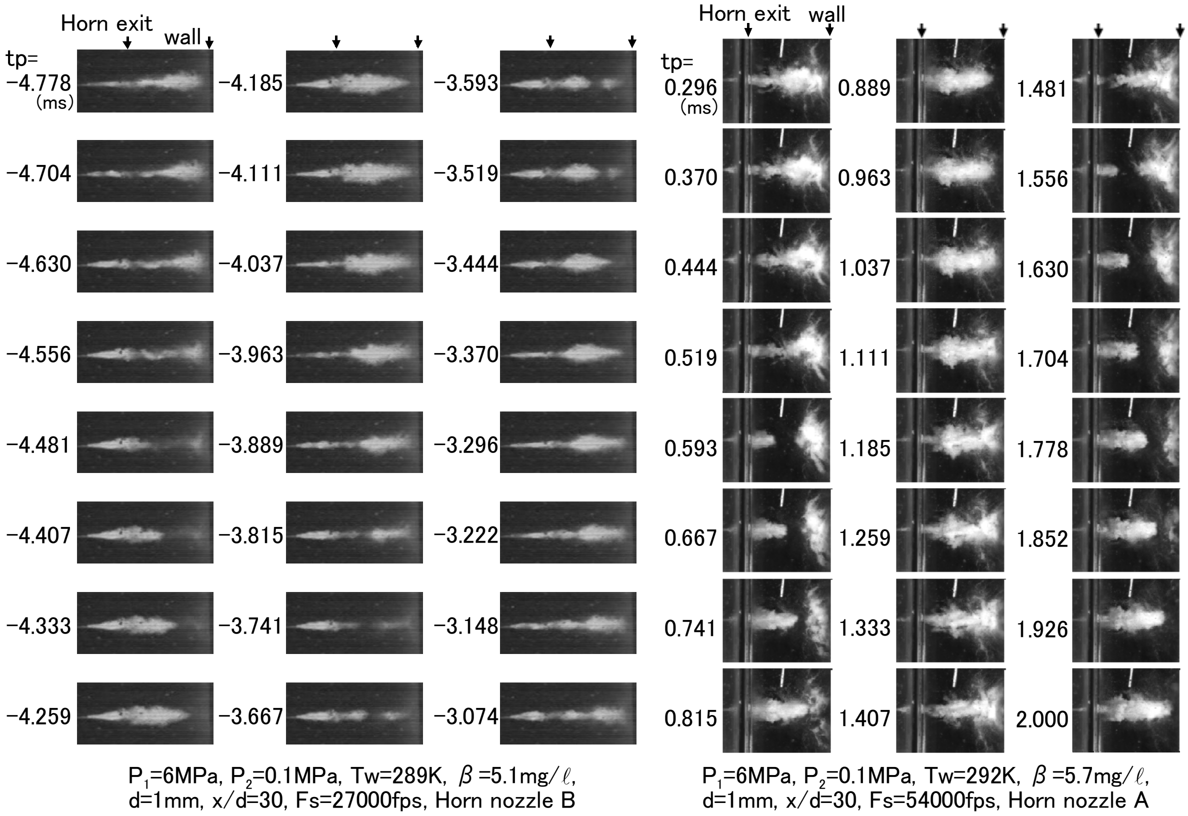

(a) Test section A (b) Test section B

Figure A: Comparison of periodic behavior of cavitating water jet between open-type test section A and constrained-test section B

appearance of cavitation cloud impinging on the wall. On the other hand, in the case of an open-type test section A it is difficult to observe the cloud behavior near the impinging wall because the impinging jet spreads toward a radial direction on the wall surface and makes a cloudy curtain to obstruct the side view. In the present experiment the constrained-type test section B was used to optically examine the behavior of cavitation cloud and the mechanism of pressure wave in the near impinging wall region.

Figure A shows the whole appearances of cavitating water jet in both the test section A and the test section B from the jet issue to the impinging stage on the wall, respectively. It is confirmed that both the cavitating water jets have a periodic unsteady character accompanied with the discontinuity of cavitation clouds. In the case of test section B the images are clear especially in the near impinging wall region though the cavitation cloud tends to expand to a transverse direction.

Appendix-B: Appearance of ring-like erosion distribution on impinging wall

Figure B shows an erosion distribution on the solid wall under the test condition of stand-off 30d where d and t depict the diameter of nozzle throat and the period of erosion test, respectively. The configuration of the erosion area appears to be ring-like or annular. It is confirmed that the annular eroded area exists roughly within the limit of z/d=±5 to ±15. It should be noticed that there is an exactly circular area of the center in a scarcely eroded state. This result means that the jet peripheral type of cavitation cloud collapse is closely related to cavitation erosion or strong cavitation impacts while the relation of the jet center-axis type is very weak.

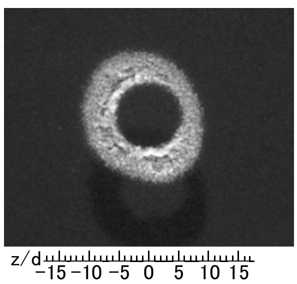

Figure B: Ring-like erosion on acrylic resin plate